Journal of Archaeological Science 52 (2014) 204–217

Contents lists available at ScienceDirect

Journal of Archaeological Science

journal homepage: http://www.elsevier.com/locate/jas

# Assessing heavy metal exposure in Renaissance Europe using synchrotron microbeam techniques

Antonio Lanzirotti [a, *], Raffaella Bianucci [b, c, d, e], Racquel LeGeros [f], Timothy G. Bromage [f, g], Valentina Giuffra [d], Ezio Ferroglio [h], Gino Fornaciari [d], Otto Appenzeller [i]

[a] The University of Chicago, Center for Advanced Radiation Sources, 9700 S. Cass Ave., Bldg. 434A, Argonne, 60439, Chicago, IL, USA
[b] University of Turin, Department of Public Health and Pediatric Sciences, Turin, Italy
[c] University of Oslo, Centre for Ecological and Evolutionary Synthesis (CEES), Department of Biosciences, Oslo, Norway
[d] University of Pisa, Department of Translational Research on New Technologies in Medicine and Surgery, Pisa, Italy
[e] UMR 7258, Laboratoire d'Anthropologie bio-culturelle, Droit, Etique & Santé (Adés), Faculté de Médecine de Marseille, France
[f] New York University College of Dentistry, Department of Biomaterials and Biomimetics, New York, NY, USA
[g] New York University College of Dentistry, Department of Basic Science and Craniofacial Biology, New York, NY, USA
[h] University of Turin, Department of Veterinary Sciences, Grugliasco, TO, Italy
[i] New Mexico Health Enhancement and Marathon Clinics Research Foundation, Albuquerque, NM, USA

ARTICLE INFO

*Article history:*
Received 13 January 2014
Received in revised form
10 August 2014
Accepted 15 August 2014
Available online 27 August 2014

*Keywords:*
Synchrotron microprobe
Heavy metals
X-ray fluorescence
X-ray absorption spectroscopy
Zoonotic visceral leishmaniasis
Neapolitan nobles
Renaissance

ABSTRACT

A number of archaeological studies have used chemical analysis of preserved, human biological tissues to assess the potential exposure of historic figures and ancient populations to heavy metals. Accurately assessing historic levels of heavy-metal body burden for these individuals based on analysis of remnant soft-tissue, hair and bone collected from preserved human remains is often complicated by the potential for post-mortem chemical modifications and contamination of the body and burial site. This study employs high-resolution, synchrotron-based elemental X-ray fluorescence mapping, tomography and absorption spectroscopy of human remains collected in an archaeological context in an effort to discriminate between heavy metals such as mercury and lead that may have been incorporated through either endogenous or exogenous processes. These methods were used to analyze bone and hair samples from Ferrante II of Aragon, King of Naples (1469–1496) and Isabella of Aragon, Duchess of Milan (1470–1524). These individuals are likely to have been exposed to generally similar levels of heavy metals in their lifetime, would have been embalmed using similar methods and the post-mortem exposure to contaminants is likely to have been similar. Although the remains from both Ferrante II of Aragon and Isabella of Aragon contain high amounts of mercury and lead, the high-resolution and –sensitivity synchrotron microprobe techniques employed in this study provide insight in to the likelihood these metals were incorporated pre-mortem rather than as ante-mortem contaminants. Although synchrotron X-ray fluorescence mapping and tomography are generally consistent with measured mercury from Isabella hair samples being endogenous in nature, the high levels of mercury seen in Ferrante II's remains are most likely related to post-mortem embalming of the corpse. However, application of microfocused X-ray fluorescence compositional mapping and lead $L_2$ edge X-ray absorption spectroscopy to bone samples collected from Ferrante II show that the measured lead is likely endogenous and the result of in-life exposure to this heavy metal.



## 1. Introduction

Modern societies appreciate the adverse (and potentially fatal) health effects of exposure to heavy metals even in small quantities. Although ancient societies understood that many of these compounds were toxic when ingested in large doses, the health consequences of long term exposure to heavy metals in ancient societies were generally unappreciated, even where heavy metal pollution may have been widespread. Several analytical techniques are available that test for an individual's potential exposure to these metals, particularly mercury (Hg) and lead (Pb). Some of the more commonly applied standard methods include live blood cell

* Corresponding author. Tel.: +1 630 252 0433.
*E-mail address:* lanzirotti@uchicago.edu (A. Lanzirotti).

http://dx.doi.org/10.1016/j.jas.2014.08.019
0305-4403/

analysis, hair mineral analysis and bone analysis. Chemical analysis of remnant bone and hair samples is an analytical technique that may be utilized by archaeologists for establishing a record of the past exposure of ancient peoples to contaminants, for evaluating past dietary habits, and as a monitor of environmental changes that may have impacted ancient peoples (Rasmussen et al., 2008). This is a particularly attractive forensic technique in archaeology since bone and hair are both likely to be well-preserved in the archaeological record.

Hair is of particular interest due to its robust structural morphology and since the endogenous incorporation of trace metals in hair potentially provides a high-resolution chronological record of exposure (Bartkus et al., 2011; Byrne et al., 2010; Egeland et al., 2009; Wilson, 2005). From an archaeological perspective, trace element analysis of hair (for Hg in particular) can potentially provide temporal biomonitoring over periods of hours, weeks or months (Kempson et al., 2012). As such it has the potential to provide a historical marker of this individual's chemical "body burden", a measure of the amount of a particular element or chemical present in the body at a given point in time. Using hair specimens to evaluate Hg exposure is a well-established clinical method and it has been shown that measured Hg levels at specific points along single hairs generally reflect the Hg blood level when the hair was formed (Nuttall, 2006; Toribara, 2001). Previous studies have established that ratios of the concentration of Hg in hair relative to Hg in blood generally range from 250 to 300. This is thought to represent a reasonable approximation for Hg hair-to-blood ratios, so that a measured Hg concentration of 1 μg/g in hair would correlate to approximately 3 μg/L blood methylmercury concentration (Clarkson et al., 2003; Nuttall, 2006). Clinical studies also have shown that Hg has a long half-life in hair and remains stable over long periods of time, again increasing the potential utility of Hg analysis of hair in an archaeological context for long-term biomonitoring. X-ray fluorescence (XRF) analysis for Hg in single strands of hair has also been shown to be particularly sensitive (and reliable) in providing a temporal record for mercury exposure that bulk hair analysis using various techniques cannot, particularly in measuring the timing of acute exposure (Marsh et al., 1987; Toribara, 2001, 1995).

Analysis for endogenous Pb in bone as a measure of in-vivo exposure has also been demonstrated to be a generally reliable method, variably applied using differing analytical techniques. Bone lead is thought to comprise 90–95% of the total body burden of Pb in adults (World Health Organization, 1972), with deposited lead persisting for years. Lead is estimated to have a half-life between 20 and 40 years in bone. It thus can serve as a cumulative biomarker of lead body burden and of chronic Pb exposure (Bleecker et al., 1995). XRF analysis of bone in particular has been shown to provide high detection sensitivity for assessing retroactive exposure (Ambrose et al., 2000; Bleecker et al., 1995). However, the degree to which bone lead levels can be used to establish a link between lead exposure and neurotoxicity remains unclear (Bleecker et al., 1997). As with hair analysis, the XRF analysis of Pb in remnant bone is highly attractive from an archaeological perspective as a measure of historical exposure of an individual over some time period prior to their death. Examples of such studies, many using synchrotron-based microprobes, include Dolphin et al. (2013), Keenleyside et al. (1996) and Martin et al. (2013, 2007).

However, evaluating historic levels of heavy-metal body burden based on analysis of remnant soft-tissue, hair and bone collected from preserved human remains can be complicated by post-mortem chemical modifications and contamination (Chevallier et al., 2006; Kempson et al., 2007, 2006; Price et al., 1992). These exogenous, post-mortem contaminants can be difficult to identify and/or distinguish from endogenous metals in archaeological samples and, when not identified, can lead to incorrect interpretations regarding historical levels of exposure. For example, heavy metals may be introduced from cosmetics used in preparing the corpse for burial, embalming materials, from the use of insecticides and fungicides during later preparation, curation, or restoration of remains and due to long-term environmental contamination from the burial site. High resolution elemental analysis techniques such as synchrotron X-ray micro-fluorescence and -spectroscopy may potentially provide a more accurate assessment of heavy metal accumulations that occurred during life by providing researchers a sensitive, spatially-resolved method to measure metal abundance, chemical form and molecular structure at relevant concentrations and at micrometer and submicrometer length scales (Kakoulli et al., 2013; Kempson and Henry, 2010).

In this study we use these techniques to study bone and hair samples collected from mummified remains of two historical individuals which have previously been reported to have potentially been exposed to heavy metals during their lifetime (D'Errico et al., 1988; Fornaciari et al., 2011), Ferrante II of Aragon, King of Naples (1469–1496) and Isabella of Aragon, Duchess of Milan (1470–1524). While circumstantial evidence suggests that Ferrante II and Isabella may have been exposed to heavy metals in life, the data has been inconclusive in establishing that the measured heavy metals are endogenous and that exposure to these toxins in life impacted their health. The goal of this study is to evaluate the potential in-vivo exposure of these historical figures to lead- and mercury-containing compounds and demonstrate the general utility of these methods for other similar studies.

During the Middle-Ages and the Renaissance exposure to heavy metals through dietary intake and medicinal uses is thought to have contributed to human absorption of these toxins (Rasmussen et al., 2008). Humans were also exposed to heavy metals through use of pewter and other lead-bearing cooking utensils, tableware and pottery, use of lead water pipes and through ingestion of foods and beverages adulterated with lead-based additives. By the 15th century, arsenic, lead and mercury were often applied to crops across Europe as pesticides and increasingly found in the environment (in water, soil and in the atmosphere) as industrial contaminants (Brännvall et al., 1999), increasing dietary exposure to heavy metals and metalloids in the general population. Exposure to heavy metals from cosmetics were also likely, such as from the use of lead-based and mercury-based (quicksilver and sublimates of mercury) whitening agents on the face (Drew-Bear, 1994). Cinnabar was included among the cosmetic darkening substances called 'browning' and was also used to dye hair.

Additionally, mercury-containing ointments, fumigations, pills and syrups are known to have been used to treat a variety of medical conditions. For example, they were used to treat the ulcers and luetic swellings that often accompanied syphilis and leprosy (Marinozzi and Fornaciari, 2005), diseases which were rampant across Europe in the 15th century. Scientific research indicates mercury-containing ointments were used to treat lice infestations (Fornaciari et al., 2011, 2009), to treat putrid ulcers, sores, warts and pocks, to treat erythema, used to remove blotches and freckles from the face and used as an anti-putrefactive balm (Marinozzi and Fornaciari, 2005). While popular rumors suggested that Ferrante II had syphilis, the historical/medical reports attributed his death to "malignant tertian malaria" (Minervini, 1923; Passero, 1780). Isabella is reported to have suffered from "dropsy" prior to her death (Pepe, 1900), an excessive accumulation of fluids in her tissue. Previous studies found high levels of mercury associated with the remains of both individuals (D'Errico et al., 1988; Fornaciari et al., 2009) which suggested that they may have been exposed to potentially toxic levels of heavy metals during their lifetime.

The individuals studied here would likely have been exposed to levels comparable to that of the general population at the time. This poses a challenge in interpreting heavy metal concentrations measured in human remains from an archaeological perspective. How best to establish that the elements measured represent endogenous metals that were accumulated in the body pre-mortem from those that were exogenous and accumulated either pre- or ante-mortem with no substantive impact to individual health? The application of high-resolution, synchrotron-based elemental X-ray fluorescence (XRF) mapping, tomography and X-ray absorption spectroscopy can provide considerable insight in this regard with varying degrees of confidence. Particularly as relates to figures of historical significance, high resolution elemental imaging and spectroscopy can clarify to what degree measured heavy metals actually relate to in-vivo exposure to environmental toxins and avoid misinterpretation of data.

## 2. Materials and methods

Samples analyzed in this study were provided from autopsies performed at the church of San Domenico Maggiore in Naples and the findings (Fornaciari, 2006, 1985; Marinozzi and Fornaciari, 2005) are summarized here. The samples studies are hair strands from both individuals, fragments of remnant muscle tissue and sections of bone from Ferrante II and an embalming sponge found in his abdominal cavity. The autopsies were performed at the church of San Domenico Maggiore in Naples in 1984. The church dates back to the beginning of the 14th century. The remains of Aragonese princes and other members of the Italian nobility are entombed in wooden sarcophagi stored in a walkway overlooking the sacristy (Supplementary Fig. S1). Ferrante II's remains were poorly preserved because of a fire in 1509 which destroyed the sarcophagus in which his mummified remains were entombed. His calculated stature was 176 cm long (Olivier et al., 1978; Trotter and Gleser, 1977); the limbs were skeletonized, the anterior cranial bones and half of the parietal bones were burned. Both feet were also burned. There were greenish discolorations over the left clavicle, humerus, radius and ulna attributed to copper oxides from metallic objects found in the coffin. Skin fragments were present on his back and hair was identified on his back, pubic region and chest. The cranial, thoracic and abdominal cavities were filled with marine sponges (*Euspongia officinalis* L.) soaked with embalming substances. The sponges had been linked to each other with rope to facilitate their immersion in the embalming fluids and to ease their subsequent deposition into the body cavities. There was evidence of lice infestation in Ferrante II's head and pubic hair (Fornaciari et al., 2009). Historical accounts indicate that Hg was used to combat itching during Renaissance (Fioravanti, 1561) but no historical reference to Ferrante's personal treatment exists.

Isabella's body was completely skeletonized, only hair, disarticulated bones and clothes were found in her sarcophagus. Her body stature was calculated to be 166 cm long (Olivier et al., 1978; Trotter and Gleser, 1977). All bones showed a dark greenish discoloration attributed to metallic oxides which leached from her crown and other metallic objects found in her sarcophagus. Analysis of a black patina found on her teeth (Fig. 1 and 2) using energy dispersive scanning electron microscopy showed this to be high in mercury (D'Errico et al., 1988). This is consistent with excretion of metabolically-absorbed mercury from the body through salivary glands. This scanning electron microscopy study also showed that the buccal surfaces of the teeth had been intensively and voluntarily abraded to eliminate the blackish Hg patina, likely for esthetic reasons, and contained little Hg. In contrast, the interdental spaces and lingual surfaces of premolars and molars (which are difficult to reach with toothpicks) were characterized by the presence of the Hg patina. It is clear from these studies that this Hg is due to in-vivo exposure. It has been speculated that the a likely source may have been anti-syphilitic treatment with mercury-containing compounds (D'Errico et al., 1988). This hypothesis was formulated because syphilis had reached epidemic proportion in Europe in the 15th century. However no scientific reports support the notion that Isabella was suffering from a luetic infection.

**Fig. 1.** The skull of Isabella di Aragon (Isabel of Aragon). Note the greenish patina most likely of metal oxides that leached over the centuries from her crown that she was found with the body.

Synchrotron-based microfocused X-ray fluorescence (μXRF), X-ray absorption spectroscopy (μXAS) and X-ray fluorescence


**Fig. 2.** The remains of Isabella's black patina on her teeth. The pre-mortem abrasions, presumably for cosmetic reasons, are also evident. Analysis of the black material (D'Errico et al., 1988) showed this black patina contains very high levels of mercury, which may be consistent with mercurial stomatitis.

computed microtomography (fCMT) analyses were conducted at beamline X26A at the National Synchrotron Light Source, Brookhaven National Laboratory (Upton, NY, USA). Compositional mapping of Pb and Hg in samples was conducted using a monochromatic X-ray beam variably tuned to 12.5 and 13.5 keV using a Si(111) channel-cut monochromator (this was done to image above and below the Pb $L_3$ absorption edge to avoid spectral overlaps with As emission lines). Monochromatic X-rays were focused to a beam size of 5 × 8 μm (V × H) using a pair of 100 mm long, elliptically-bent, Rh-coated silicon mirrors in a Kirkpatrick–Baez geometry. Photon flux within this spot at these incident beam energies varied between 3 and 5 × $10^9$ photons per second. X-ray fluorescence spectra were collected using two single-element Vortex-EX silicon-drift-diode detectors and one 4-element Vortex-ME4 silicon-drift-diode detector (Hitachi High-Technologies Science America, Inc.). Compositional maps were collected in a continuous scan mode as described in Lanzirotti et al. (2010). Elemental abundances were calculated using the NRLXRF program (Criss et al., 1978) following the general methodologies described in Lanzirotti et al. (2008), Sutton et al. (2002) and Zhang et al. (2012).

Single strands of unwashed hair were analyzed (unsectioned) using synchrotron μXRF methods and elemental abundances were calculated based on comparison to a thin-film standard reference material (SRM 1833) and standard reference material NIES No.5 (human hair) that was measured prior to the collection of each data set to establish elemental sensitivities. Sample thicknesses were calculated by measuring X-ray attenuation through the sample in a photodiode detector and assuming a uniform absorption coefficient for each emission line. We used an absorption coefficient appropriate for cellulose, which we assume is a reasonable proxy for the absorption coefficient of human hair. Measured abundance of Hg in NIES No.5 gives excellent agreement with the certified values.

For bone analysis, bone was embedded in polymetylmethacrylate and sectioned to 60 μm thickness on to an Exakt® plastic substrate. XRF analysis of materials ensured substrates and embedding media were trace-element clean. Elemental abundances for bone were calculated using a standardless fundamental parameters approach (Kanngießer, 2003; Lanzirotti et al., 2010), referenced to measured Ca Kα emission intensities and assuming a standard “bone” bulk chemical composition. For fCMT analysis, individual hair fragments were mounted on a motorized Huber goniometer-head and centered with respect to the rotational axis of the sample stage. Full energy dispersive spectra were then collected from each sample as it was scanned through the focused beam horizontally in a continuous (fly-scan) mode. X-ray absorption through the sample was also measured simultaneously in a photodiode placed downstream of the sample. Data were collected over 180 degrees of rotation and spectra were accumulated every 3 μm of motion through the beam (one pixel) with a scan rate of 250 msec per pixel. Sinograms (angle vs. horizontal position) were generated for each element of interest by extracting the peak intensity from the full spectra for a representative X-ray fluorescence emission energy (i.e Hg Lα, Pb Lα, Zn Kα, etc.) Tomographic slices of the X-ray fluorescence intensity and X-ray absorption through each hair were then computationally reconstructed using filtered back-projection using procedures similar to those described in Kim et al. (2006), Punshon et al. (2009) and Zhang et al. (2012). The reconstruction algorithms are incorporated in beamline specific software (http://www.bnl.gov/x26a) written in IDL (Interactive Data Language, Exelis VIS). Given the small sample diameter and low material density, the influence of x-ray self-absorption by the matrix for the X-ray emission lines being imaged was found to be negligible, therefore no self-absorption corrections (such as those employed in Zhang et al. (2012)) were deemed necessary.

Analysis of the chemical state of the bone Pb was conducted using microfocused X-ray absorption near edge structure (μ-XANES) spectroscopy at beamline X26A. XANES provides an element-specific spectroscopic analysis of the partial density of the empty states of a molecule and can provide a measure of the absorbing atom's formal valence and coordination environment. Spectra were collected by scanning the incident beam energy through the Pb $L_2$ absorption edge (15,200 eV). The $L_2$ edge was used rather than $L_3$ primarily to avoid spectral overlaps in fluorescence mode. Again, the incident X-ray energy was tuned using a Si(111) channel-cut monochromator. The XANES spectra from a thin section of rib from Ferrante II were collected in fluorescence mode and compared with measured spectra of several reference compounds including metallic Pb, $PbSO_4$, $PbCl_2$, $Pb_3(PO_4)_2$, PbO, $PbCO_3$, and Pb-substituted hydroxyapatite (Pb-HA). All reference compounds except metallic Pb (run as a thin foil) were prepared as layered powders on scotch tape (Newville, 2014) and analyzed in transmission-mode, with the exception of the Pb-HA which was analyzed in fluorescence-mode, at the Pb $L_2$ edge using a defocused 0.3 × 1.0 mm beam. The transmitted signal was measured in a photodiode downstream of the sample. Fluorescence-mode XANES monitored the intensity of the Pb Lβ emission line and, for the bone samples, 15 scans were summed to improve signal-to-noise. Each scan represents approximately 10 min of accumulation time. Over the total ~150 min of accumulation time no changes were observed in the XANES spectra (either in edge position or resonance shape) that would be indicative of radiation induced changes in valance state or speciation over time. Energy calibrations are based on the $L_2$ edge position of a Pb reference foil and the foil was rerun periodically to monitor for any potential drift in energy over time. XANES spectra were analyzed using the ATHENA software package (Ravel and Newville, 2005) and normalized to an edge jump of one.

Powdered bone fragments from samples of Ferrante's rib and vertebra and from Isabella's vertebra were examined by Thermogravimetric Analysis (TGA; SDT Q600, TA instruments, New Castle, DE), Inductively Coupled Atomic Emission Spectroscopy (ICP-AES; Thermal-Electron Incorporated, Franklin, MA) and Fourier transform infrared spectroscopy (FTIR; Nicolet 550 Series II, Thermo Scientific, Walthan, MA). Analyses were performed at the New York University College of Dentistry Department of Biomaterials and Biomimetics. For TGA and ICP-AES analysis, samples were powdered and dissolved in an acidic buffer solution of 0.1 M KAc at 37 °C and a pH of 6. Dissolution rate of the mineral phase in acidic buffer was also compared. TGA and ICP-AES results are presented in Table 1. For FTIR analysis, a sample pellet was prepared by mixing 10 mg of the sample with 250 mg KBr (IR grade). The pellets were pressed at 10,000 psi using a hydraulic press (Carver laboratory press, mode C, ser. No. 33000-577, Fred S. Carver, Inc.).

**Table 1**
Thermogravimetric Analysis (TGA) and Inductively Coupled Atomic Emission Spectroscopy (ICP-AES) analyses of powdered bone from Ferrante II and Isabella.

| | Ferrante | Isabella |
|---|---|---|
| **TGA (wt. %)** | | |
| Organic | 26.0 | 24.0 |
| $H_2O$ | 9.2 | 9.4 |
| $CO_3$ | 7.4 | 8.6 |
| Total mineral | 64.4 | 66.4 |
| **ICP-AES (wt. %)** | | |
| Ca | 31.73 | 30.85 |
| P | 14.97 | 16.54 |
| Mg | 0.17 | 0.28 |
| Pb | 0.0098 | 0.0110 |
| F | 0.000 | 0.008 |

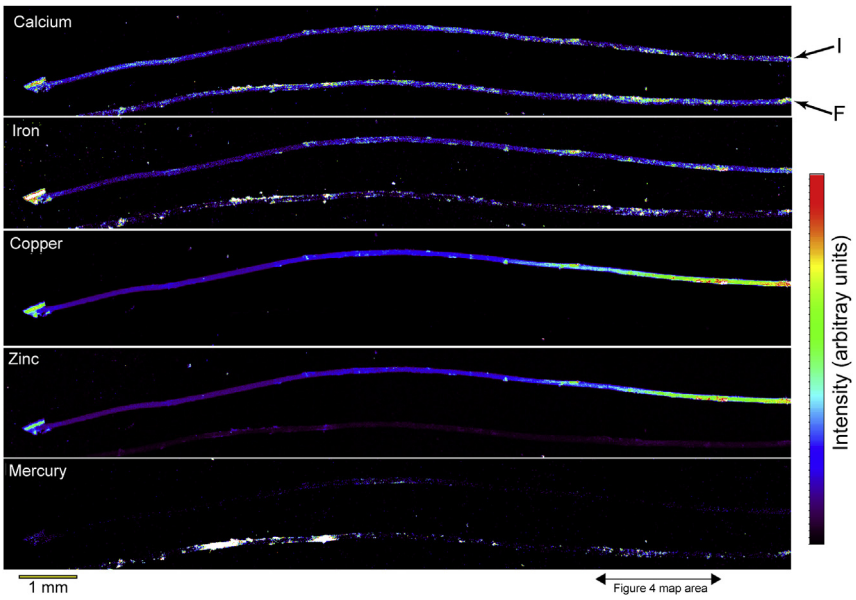


**Fig. 3.** Synchrotron μXRF compositional maps of hair from Isabella and Ferrante II. Shown are μXRF compositional maps of selected elements for two single strands of hair from Isabella and Ferrante II. Hairs are oriented so that the root of each hair is to the left. In each image the uppermost hair is from Isabella (labeled "I") and the bottom from Ferrante (labeled "F"). The intensity scaling shows variations in calculated relative elemental concentrations (based on changes in X-ray fluorescence intensity) with the highest intensity in each compositional map representing the highest concentrations measured for each elemental emission line. The scaling (referenced to the relative scale bar shown to the right) is thus not comparable between elements (i.e. copper vs. mercury). Summed energy dispersive spectra for the Isabella hair for the area between X distance 6.1 and 7.2 mm and for Ferrante hair for the area between X distance 5.0 and 5.9 mm are shown in Supplementary Fig. S3. The maps were collected in a continuous scan mode with a 7 μm pixel size and an accumulation time of 100 msec per pixel and a 1 mm scale bar is shown at bottom. Also shown is the area that is mapped at higher resolution for the Isabella hair in.Fig. 4.

Since malaria and zoonotic visceral leishmaniasis (ZVL) were rampant in central and southern Italy at that time (Bianucci et al., 2012; Fornaciari et al., 2010; Nerlich et al., 2012), paleoserological tests (immunoassays for ZVL and malaria and Western Blot SDS-PAGE for ZVL) were carried out to ascertain whether one of those infectious diseases might have been the cause of the recurrent fevers in the nobles. These results are presented and described in Supplemental Text S1 and Supplementary Fig. S2.

## 3. Results

### 3.1. Trace elements in hair

Determination of mercury levels in hair samples from Ferrante has previously been reported in Fornaciari et al. (2011), measured by Atomic Absorption Spectroscopy (AAS) followed by Flame Emission Spectrophotometry (FES) using the hydride method. A

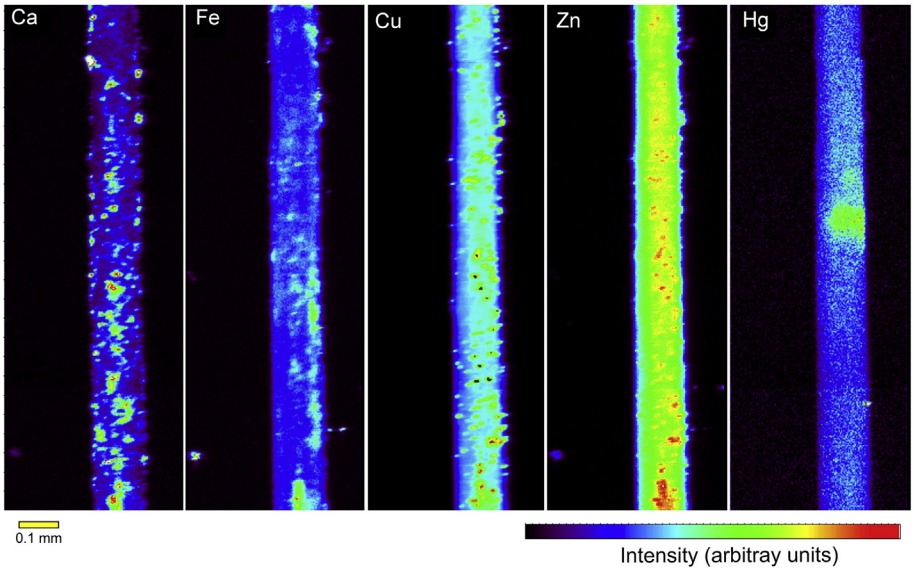


**Fig. 4.** High resolution μXRF compositional maps of hair from Isabella. μXRF compositional map of Ca, Fe, Cu Zn and Hg in 1.3 mm long section of hair from Isabella. This is a higher spatial resolution image of the same hair from Isabella shown in Fig. 3 centered at the 11.7 mm from the left edge of Fig. 3. Map was collected in a continuous scan mode with a 3 μm pixel size and an accumulation time of 200 msec per pixel, a 0.1 mm scale bar is also shown. Note that with the exception of two relatively isolated areas of localized high Hg, the elemental abundance for Hg varies smoothly.

mercury concentration of 827 ppm was found in Ferrante's hair and 411 ppm in Isabella's hair. Microfocused XRF compositional mapping of relative concentrations for calcium, iron, copper, zinc and mercury in hair from Ferrante and Isabella (Fig. 3; Supplementary Fig. S3) shows that while concentrations of Ca in both hairs are generally similar, Fe is elevated in the Isabella hair strand by a factor of 1–2× (mean abundance) while Zn and Cu are higher by a factor of ~3× and 100× mean concentration, respectively. Mercury is higher in Ferrante's hair by between 7× and 10× mean abundance, consistent with the bulk AAS results, but often displays localization in spatially resolved "hot-spots" of significantly elevated abundance, up to 1000× the maximum value observed in Isabella hair strands. The distribution of Hg in Ferrante's hair (and to some degree Fe and Ca as well) does not vary smoothly in abundance along the length of the hair. The distribution of all these elements in Isabella's hair appears less dominated by hot-spots, with elemental distributions showing relatively smooth gradations in concentration along the length of the hair. This is more apparent in smaller scale compositional maps of these elements for Isabella's hair strand (Fig. 4) although occasionally some localized, rapid changes in Hg abundance are observed (Fig. 4 at ~0.75 mm Y distance).

Plots of the elemental concentrations of Zn and Hg calculated in a spatially resolved manner along the length of each hair are shown in Fig. 5, calculated assuming that each element is uniformly distributed within the hair and using the measured diameter of the hair at each position in the map to calculate a cylindrical volume. As discussed previously, the observation that many elements, Hg in Ferrante's hair strand in particular, are present as spatially localized "hot-spots" indicates this is in reality not a realistic assumption for some of the elements measured. However, this is a useful exercise for visualizing the absolute differences in metal concentration between the two hairs. In the Isabella hair strand there is a general positive correlation between Zn and Hg content and Zn (mean of 419 ppm) is roughly 3 times higher than that measured in Ferrante's hair strand (mean of 126 ppm). The mean Hg content is significantly higher in Ferrante's hair strand (305 ppm) compared to Isabella's (14 ppm). The figure also shows that localized hot-spots of Hg exceed the observed Hg in Isabella's hair by up to a factor of 1000×.

Figs. 6 and 7 show reconstructed tomographic slices of the distribution of Ca, Fe, Cu, Zn and Hg in a fragment of Isabella's and Ferrante's hair, respectively, collected using fCMT. Structurally, hair can be subdivided into three concentric compartments when viewed in cross-section; from the center outward hair can be subdivide into the medulla, cortex and cuticle with the hair cortex constituting roughly 90% of the total hair mass (Bertrand et al., 2003). In the Isabella hair fragment these elements are observed in all three compartments, within the spatial resolution of the tomographic reconstruction, with the highest metal abundances being found distributed within the hair cortex. In the tomographic reconstruction of the Ferrante hair fragment, the highest concentrations of all these elements, but particularly Ca, Fe and Hg, are in small, localized areas on the hair surface. This is consistent with what is observed in the longitudinal mapping of the hair strands. The high X-ray absorption of these localized spots in the reconstructed X-Ray absorption tomogram also shows that these elevated metal areas have a higher X-Ray attenuation coefficient (and thus likely higher density) than the background human hair. These observations strongly suggest that these elevated concentrations on the hair surface represent high-density, metal-rich, exogenous components.

### 3.2. Trace elements in bone, muscle and embalming sponge

To evaluate potential long-term metal accumulation, thin sections prepared from samples of Ferrante's rib and third lumbar

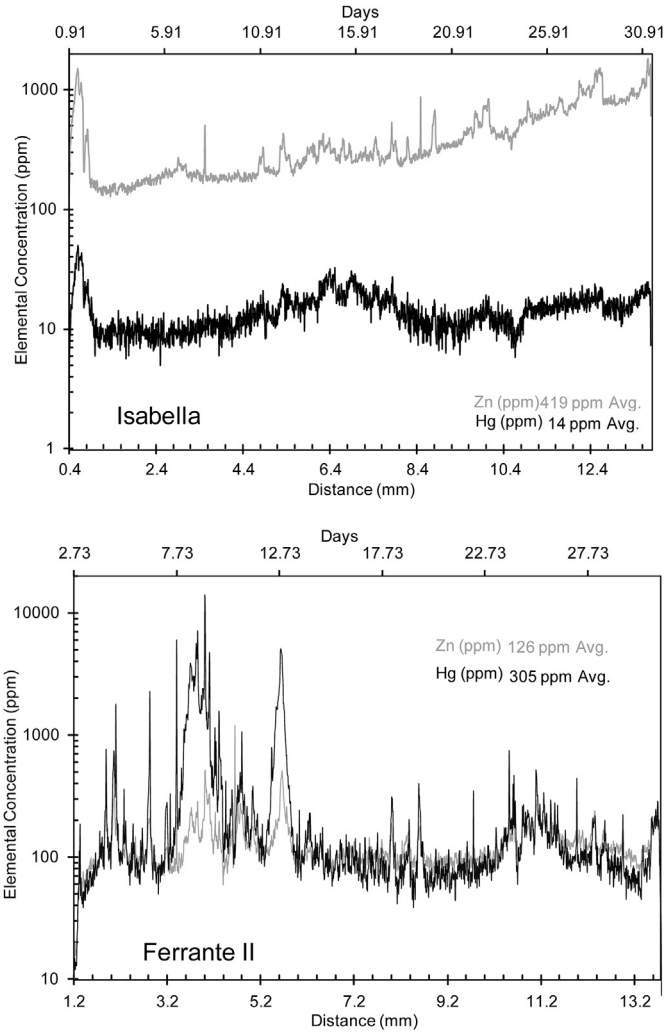


**Fig. 5.** Hg and Zn abundances along hair length. Spatially resolved concentration (in parts per million) of Hg (black curve) and Zn (gray curve) along the length of each hair shown in Fig. 3. The bottom horizontal axis of each figure shows both distance measured along the hair in mm's and the upper axis presents estimated days of hair growth from the hair root assuming an average growth rate of 0.4 mm/day. Presenting these results in concentration units assumes the measured metals are metabolically incorporated as part of the hair structure. In other words, human hair with a density of approximately 1.32 g/cm$^3$. This would not be a reasonable assumption for a case where Hg is actually and exogeneous component on the hair surface.

vertebra were analyzed by μXRF (Figs. 8–10) and ICP-OES (Table 1). A powdered sample of vertebra from Isabella was examined by FTIRC, TGA and ICP-OES (Table 1). Microfocused XRF analysis was also conducted of a sample of psoas muscle obtained from Ferrante's mummy and a marine sponge retrieved from the mummy's abdominal cavity (Fig. 11).

FTIRC analysis of bulk bone samples collected from Isabella found no evidence for mercury accumulation. This is consistent with epidemiological and toxicological studies that show that mercury tends not to accumulate within bone even for workers occupationally exposed to high levels of mercury in either a vapor or methylated form (Friberg and Vostal, 1972; Lindh et al., 1980; Skerfving et al., 1987). Synchrotron μXRF mapping also showed no evidence of Hg accumulation within areas clearly identifiable as bone in either the Ferrante rib or vertebra sections (Figs. 8 and 10). However, on the outermost surface of the rib a discontinuous band of elevated Hg up to 50 μm in thickness is observed. Higher resolution compositional maps of three of these areas are shown in

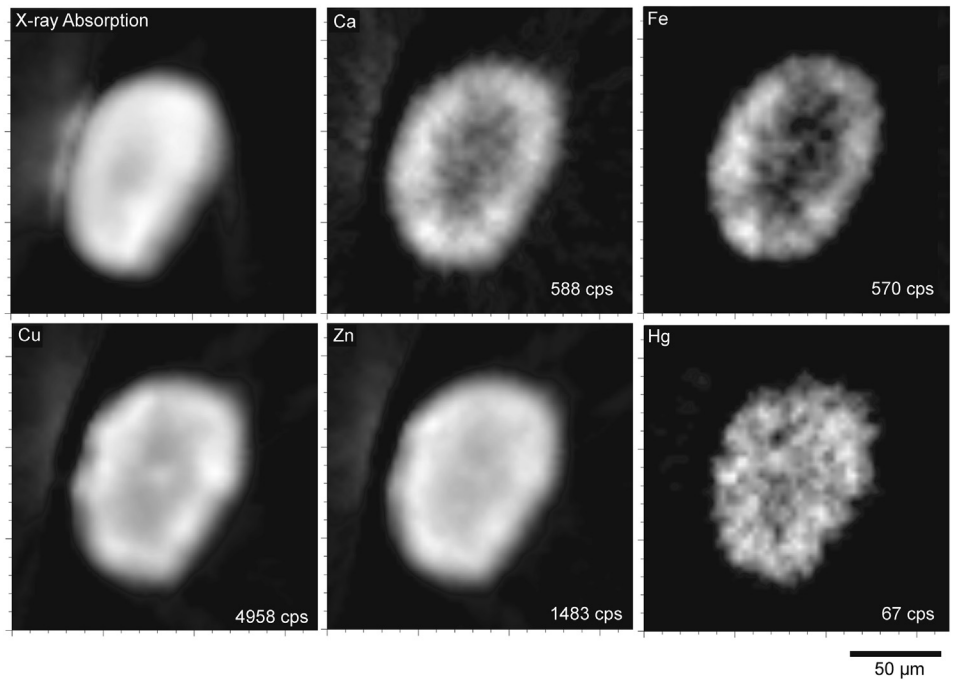


**Fig. 6.** Synchrotron XRF and absorption computed microtomography for a fragment of Isabella's hair. The upper left image shows the reconstructed slice (cross-section) of the X-Ray attenuation through the hair (to visualize variations in hair density and measured in a photodiode downstream of the sample) and the other images show tomographic reconstructions of the X-ray fluorescence intensity of Ca Kα, Fe Kα, Cu Kα, Zn Kα and Hg Lα emission lines. Image is scaled to the maximum intensity in each image and each image is annotated at the lower right with the highest count rate measured for the particular emission line in the individual tomographic slice in units of counts per second (cps). Also shown is a 50 μm scale bar.

Fig. 9. These maps show that these Hg enriched areas do not correlated with Ca (or Pb) and are thus discontinuously distributed on the bone surface. We have insufficient information to determine if this represents Hg in tissue that may be adhering to the bone or an exogenous contaminant on the bone surface from embalming.

Synchrotron μXRF mapping also shows that Pb is present throughout the rib and vertebra sections analyzed. Integration of Pb concentrations in the areas imaged using μXRF gives an average Pb concentration of 170 ppm in the rib section and 88 ppm in the vertebra. ICP-OES and FTIRC analyses of Pb in powdered bone

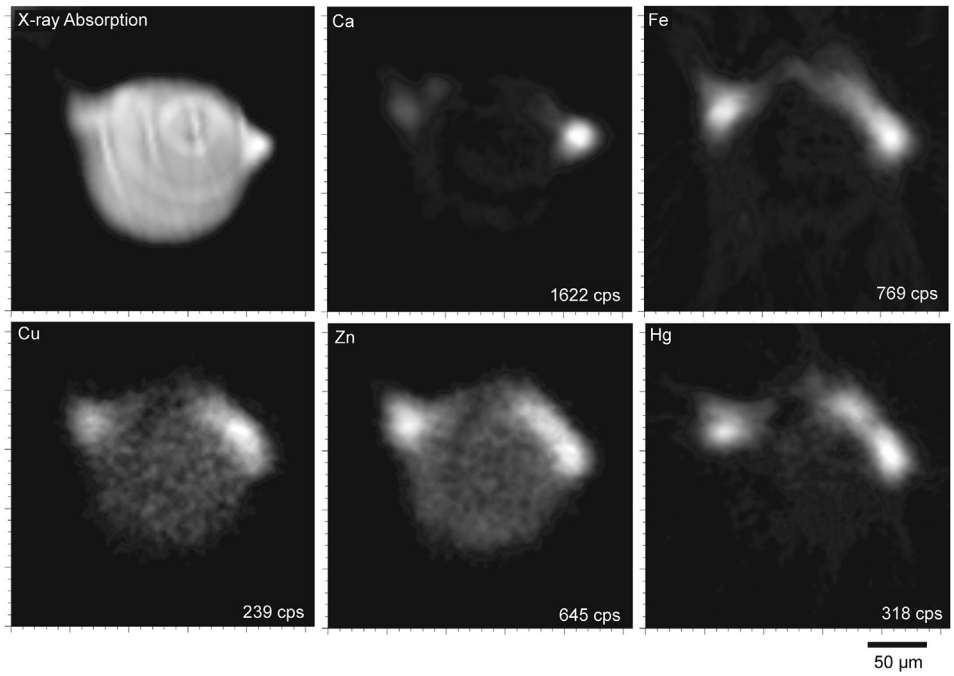


**Fig. 7.** Synchrotron XRF and absorption computed microtomography for a fragment of Ferrante's hair. X-ray fluorescence computed microtomography data collected under same run conditions described in Fig. 6 and plotted in an identical manner. Note that unlike Isabella's hair (Fig. 6), the metals are most highly concentrated in localized spots on the hair surface and that the maximum Hg counts are a factor of 4.7 times higher than in the tomographic slice of Isabella's hair strand. Cu and Zn, however, are significantly lower.

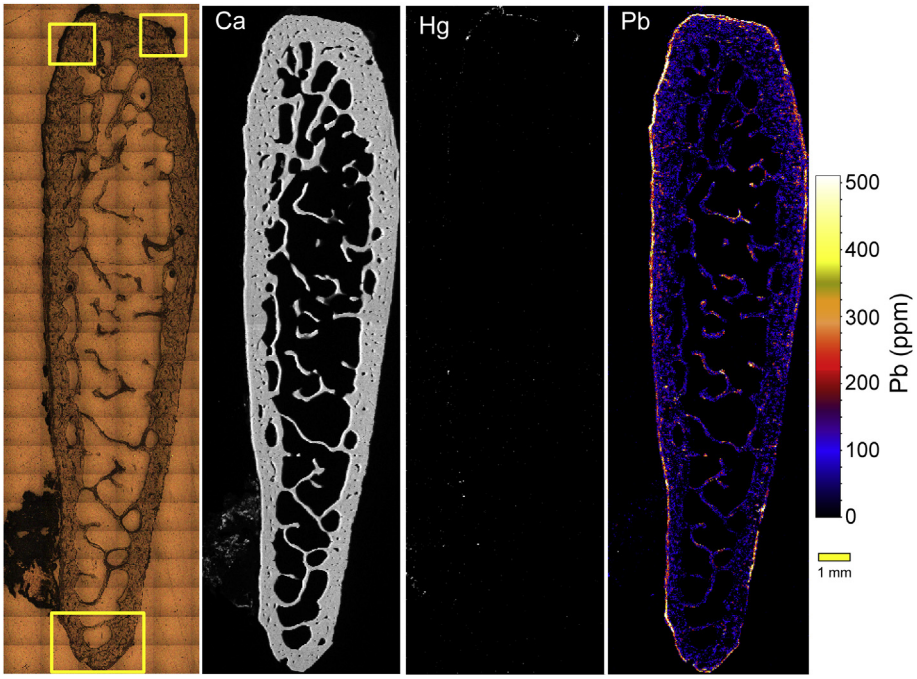


**Fig. 8.** Synchrotron μXRF compositional maps of rib section from Ferrante II. (Left) Reflected-light photomicrograph of the thin section of rib (Ferrante II) analyzed using μXRF compositional mapping. The three yellow squares show the locations of the more spatially resolved analysis presented in Fig. 9. (Right – Ca, Hg, Pb) X-ray fluorescence compositional maps of Ferrante rib section for Ca, Hg and Pb. Map was collected in a continuous scan mode with a 12 μm pixel size (1 mm scale bar is shown) and an accumulation time of 50 msec per pixel. The Ca and Hg maps show intensity of the Ca Kα and Hg Lα emission lines, respectively, scaled to the highest observed intensity for each element. The Pb map (farthest right) is shown in concentration units (ppm). Note that Ca is generally uniform in distribution throughout the bone, that the highest levels of detectable Hg are as small localized areas on the bone surface, and that Pb is easily detectable throughout the one but slightly elevated at bone margin. (For interpretation of the references to color in this figure legend, the reader is referred to the web version of this article.)

samples (Table 1) provide Pb concentrations of 98 ppm in Ferrante's bone and 110 ppm in Isabella's, consistent with the results obtained via μXRF. Pb concentrations in a ~80–100 μm wide band at the periosteal margin of the bone are 3–10 times higher than that observed for interior bone and the observed elevation is seen at the entire periphery of the sectioned bone, similar to observations from other studies (Meirer et al., 2011; Zoeger et al., 2005, Zoger et al., 2006), both with respect to the level of Pb enrichment and the thickness of this zone. These studies interpret this pattern as highly specific accumulation of Pb at metabolically active mineralization fronts of the bone. High resolution imaging of the Pb distribution in these bone sections (Fig. 9 middle and right) also shows that many (although not all) of the osteons are enriched in Pb relative to the surrounding bone.

Synchrotron XRF analysis of the psoas muscle sample from Ferrante also contained measurable Pb (not quantified), but no detectable Hg was found. Conversely, the marine embalming sponge contains notable levels of mercury and high levels of copper and halogens such as chlorine and iodine (see Fig. 11). Although absolute elemental concentrations in the sponge were not quantified, the measured Cl Kα and I Lα emission intensities are consistent with an elemental I/Cl ratio of ~1.5. The I/Cl ratio would be inconsistent with that found in seawater, which is on the order of $3 \times 10^{-6}$ (Barkley and Thompson, 1960), although some marine sponges can naturally incorporate high amounts of I (Wheeler and Mendel, 1909). However, the observed high ratio of I to Cl coupled with the high levels of Fe, Cu and Hg measured in this sponge leads us to speculate that we may partly be measuring residues of the embalming resins that were used. The presence of Hg in the sponge is consistent with previously reported data (Fornaciari et al., 2011) and with known embalming practices for other Aragonese mummies (Marinozzi and Fornaciari, 2005) and consistent with known Medieval and Renaissance mummification practices (Charlier et al., 2013).

Microfocused XANES spectroscopy was undertaken to constrain the chemical form of the Pb in the bone sections (Fig. 12). XANES spectra were collected for an interior area of bone with lower Pb concentrations (labeled point "XAS Center" on Figs. 9 and 10) and for an exterior region at the periosteal margin with elevated Pb content (labeled "XAS Margin"). We constrain the chemical species by comparing the spectra measured in bone samples to those from reference compounds. Constraining the Pb species in the bone is done by qualitative comparison of the XANES region of the collected spectra to that of the reference compounds. The confidence with which the species can be identified using this fingerprinting approach is dependent on the appropriateness of the reference compounds, but inappropriate species can be confidently excluded. Comparison of the "XAS Margin" spectra to that collected from "XAS Center" shows that they are virtually indistinguishable (residual sum of squares difference of 0.0047). Thus, based on these results it seems likely that the molecular speciation of Pb in both locations is the same. When compared to our reference compounds, the bone XANES spectra are almost identical to that measured in the synthetic, Pb-substituted hydroxyapatite reference compound, giving a residual sum of squares difference of 0.0059. This observation is consistent with other studies of Pb binding in bone (Meirer et al., 2011) where $Pb^{2+}$ substitutes for $Ca^{2+}$ in the hydroxyapatite structure.

## 4. Discussion

Previously published bulk analysis of hair from the mummy of Ferrante II indicated that it tested positive for mercury (Fornaciari et al., 2011, 2009). After thorough washing and cleaning to

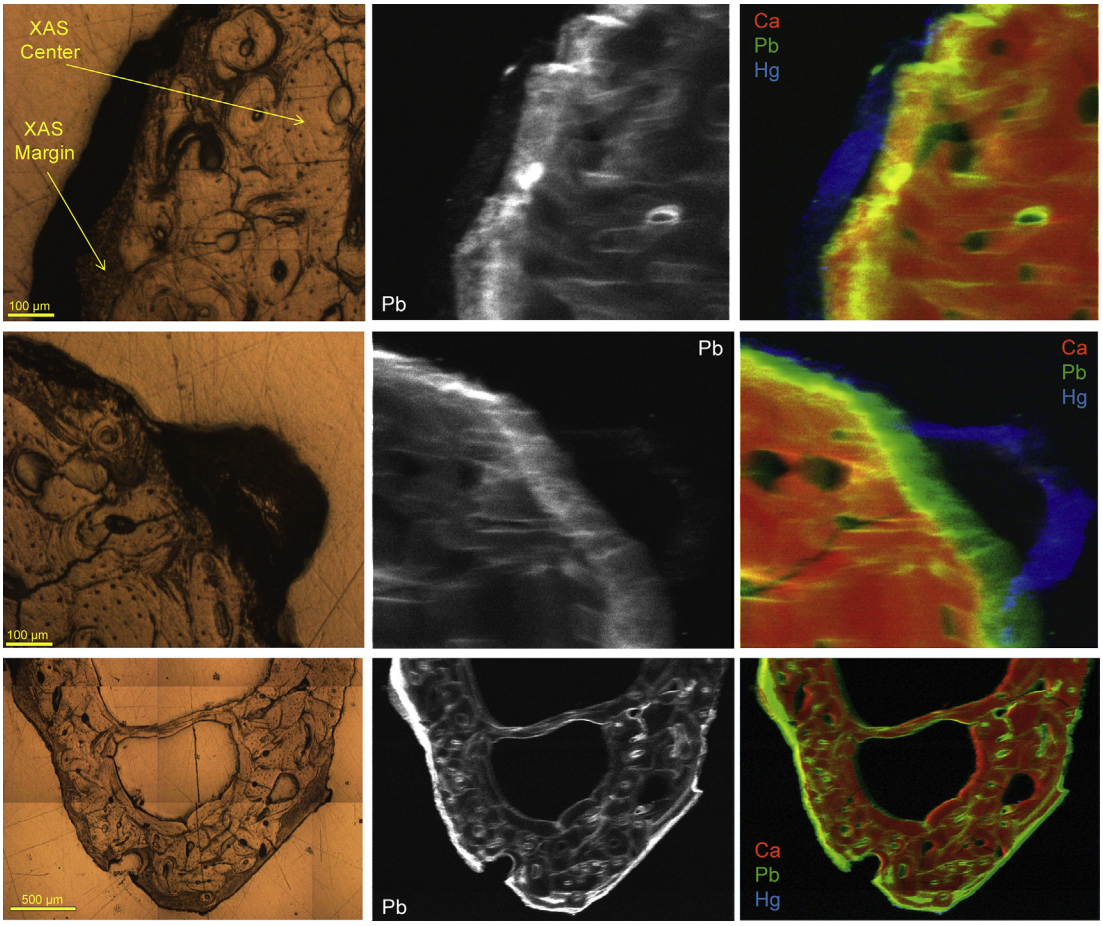


**Fig. 9.** Synchrotron μXRF compositional maps of rib section from Ferrante II. Reflected light photomicrographs (left column) and μXRF compositional maps (middle and right columns) of the localized areas defined in Fig. 8 for the Ferrante rib section. The middle column of maps show the distribution of Pb alone. The compositional maps to the right show relative distributions of Ca, Hg and Pb superimposed in red, green and blue (relative intensities are arbitrary). Maps were collected in a continuous scan mode with a 3 μm pixel size and an accumulation time of 100 msec per pixel (relative scale bars are inset on each visible light image). The figure also notes as points labeled "XAS Center" and "XAS Margin" where Pb μXANES data were collected to evaluate Pb molecular speciation. Pb compositional maps show that many of the osteons are enriched in Pb relative to the surrounding bone and that The Pb concentration increases at the bone margins. Areas of detectable Hg appear localized in areas surrounding the bone.

remove surface contaminants using 0.2% Triton- X and then rinsed several times with double distilled water (Bianucci et al., 2008), mercury was also detected in the rinsing water (Fornaciari et al., 2009). These previous studies also indicated that the mummified remains showed evidence of lice infestation. Historical records confirm the use of mercury solutions and ointments for the hair at the end of the 15th century, both for esthetic and for therapeutic purposes such as in treating pediculosis (Fioravanti, 1561). The

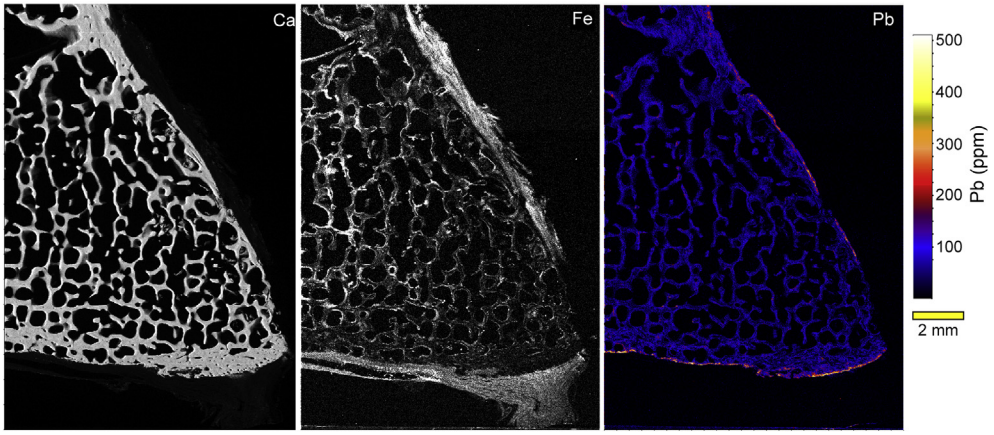


**Fig. 10.** Synchrotron μXRF compositional maps of vertebra section from Ferrante II. X-ray fluorescence compositional map of portion of Ferrante vertebra section for Ca, Fe and Pb (as described for Fig. 8). The Ca and Fe maps show intensity of the Ca Kα and Fe Kα emission lines, respectively. The Pb map is shown in concentration units (ppm) and a 2 mm scale bar is shown. As in Fig. 8, Pb is detectable throughout the bone and elevated at the bone margins.

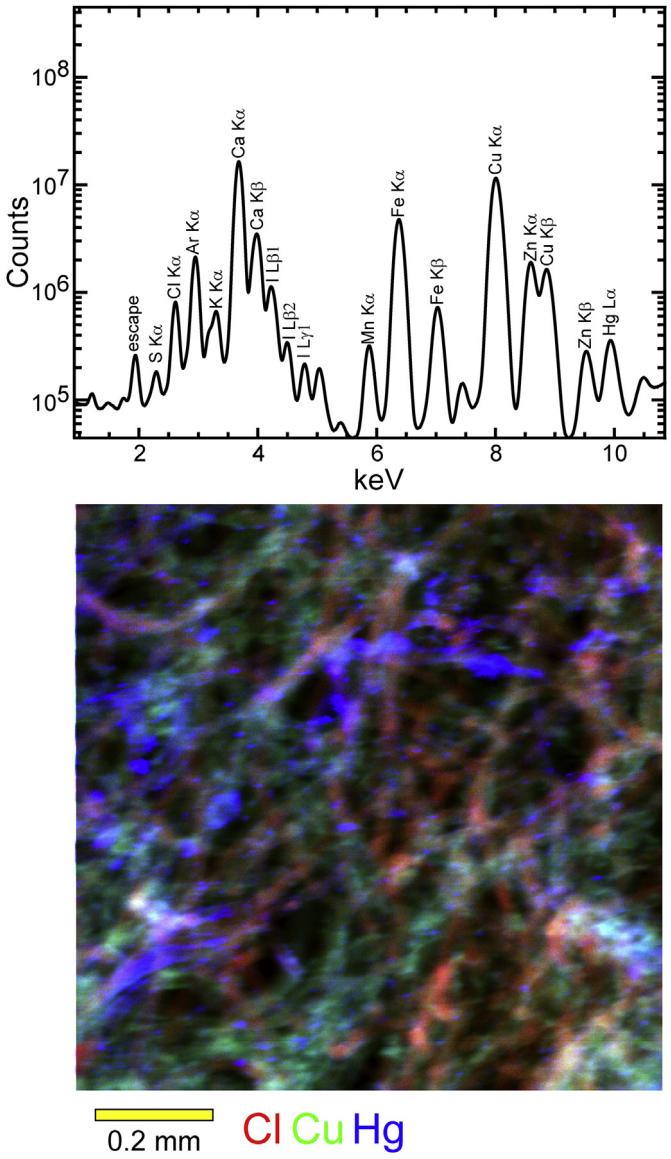


**Fig. 11.** Synchrotron XRF spectra and compositional map of Ferrante embalming sponge. (Top) Energy dispersive XRF spectra of vegetable embalming sponge removed from Ferrante's body, vertical axis is measured XRF counts vs. emission energy in keV. This is a summed spectra derived from the 1 $mm^2$ compositional map below. (Bottom) Compositional map of Map shows relative distributions of Cl, Cu and Hg in red, green and blue (relative intensities are arbitrary, 0.2 mm scale bar is shown). Note that the three elements do not correlate spatially, suggestive of differing distribution within the sponge. While Cl Kα has notable lower emission energy, Cu Kα and Hg Lα are energetic enough to be disimilarly detectable through the entire sample thickness.

serologic investigation presented here (Supplemental Text S1; Supplemental Fig. S2) also demonstrates that both Ferrante and Isabella tested positive for zoonotic visceral leishmaniasis (ZVL), a widespread infection in central and southern Italy during the Renaissance. Symptoms displayed by immune-suppressed individuals affected by active ZVL (i.e. gingivitis, tongue ulcerations) would likely have been treated in both individuals with mercury containing solutions as was usually done in cases of individuals suffering from syphilitic lesions.

A daily average methylmercury intake of 0.1 μg per kg body weight per day is estimated to result in hair mercury concentrations of roughly about 1 μg/g (World Health Organization, 2008). If the bulk Hg concentrations measured (827 ppm in Ferrante's hair and 411 ppm in Isabella's hair) reflect metabolized Hg it would require absorption in excess of 2 mg of methylmercury per day. The World Health Organization sets a standard for the upper tolerable level of mercury in hair as 5 ppm (World Health Organization, 1972).

However, both the μXRF mapping and microtomography analysis of a strand of Ferrante scalp hair show that the highest levels of Hg are localized to the hair surface, rather than within the hair itself. No mercury is detected by μXRF analysis of Ferrante's ileopsoas muscle. The chemical analysis of the embalming sponge retrieved from the abdominal cavity shows significant levels of Hg, Cu and I, likely measuring the chemical composition of the embalming resins used. Although Hg is not observed within sections of Ferrante rib and vertebral bone (at the detection limits of the synchrotron XRF microprobe), some localized areas of elevated Hg are found on the outermost portion of the rib section. We speculate this may represent Hg associated with remnants of the vegetable sponges used to fill Ferrante's abdominal cavity during embalming. This would be consistent with the autopsy observations that the cranial, thoracic and abdominal cavities were filled with sponges which had been soaked with resinous substances. Autopsy also showed that a hard, blackish layer made out of vegetable sponges soaked with resins overlapped a reddish clay layer that covered the deepest thoracic and abdominal cavities. This material may be the source of the Hg found at the bone surface. It thus seems likely that the majority of Hg measured in this study both in hair and on bone surfaces from the Ferrante mummy is exogenous and the result of post-mortem accumulation of the metal during the embalming process.

The distribution of Hg in Isabella's hair differs from that observed in Ferrante's scalp hair, however. The μXRF mapping shows mercury to generally vary smoothly in concentration along the hair shaft and tomography shows that it is elevated within the hair cortex, although the tomographic reconstruction lacks the spatial resolution to evaluate if Hg is specifically associated with melanin clusters in the cortex as described by Kempson et al. (2009). Although some small areas of localized, elevated Hg content are visible in the longitudinal mapping, they are much less significant than those observed in Ferrante's hair. This may be consistent with endogenously incorporated Hg. Evaluating the relative differences in elemental distribution of hairs coated in arsenic-containing preservatives (Kempson et al., 2009) compared to the metal distribution in the hair of mice intravenously administered metals (Kempson et al., 2012) shows that acute metal(loid) exposure can potentially be distinguishable from metal(loid)s used as preservatives that tend to distribute through hair very evenly, but not easily. While it may be expected that chronic exposure to Hg would provide a generally even (or smoothly varying) longitudinal distribution within hairs analyzed, the same can result from metals introduced externally from preservatives, cosmetics, etc. Also, synchrotron XRF imaging of the distribution of various trace elements in microtomed sections of hairs attributed to Marie de Bretagne (1424–1477) in Orléans (Loiret, France) note similar cross sectional distribution of Pb (Bertrand et al., 2014) as to that described here for Hg in Isabella's hair. The cross-sectional imaging in the Bertrand et al. study showed that Pb in washed hairs is concentrated in the cuticle and the outer cortex of the hair fiber. Their interpretation is that this represents exogenous Pb introduced from the leaching of the sheets of the coffin by running waters and binding to lipids at the hair surface, endocuticle, and the cell membrane of the cortex. Thus the observation alone that Hg is not restricted to the outermost surface of the hair, as we observe in Ferrante's hair, may be insufficient for establishing its endogenous incorporation.

The analysis of the black patina found on Isabella's teeth reported in D'Errico et al. (1988) was also found to be high in mercury,

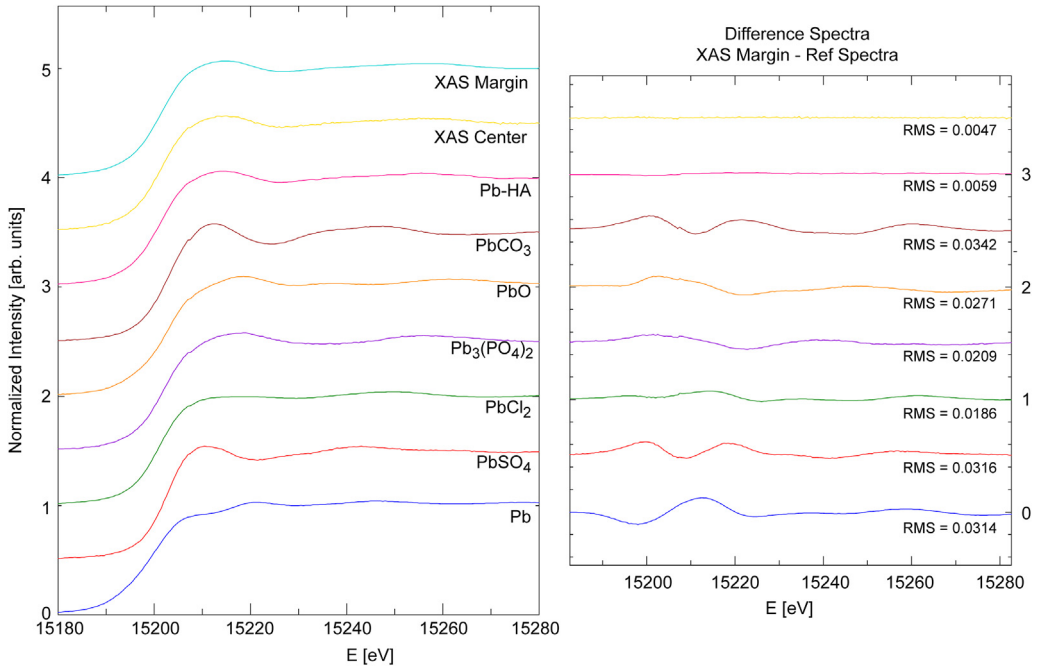


**Fig. 12.** Pb L3 μ-XANES data from Ferrante bone and reference compounds. (Left) Pb L2 μ-XANES spectra for the reference compounds Pb, $PbSO_4$, $PbCl_2$, $Pb_3(PO_4)_2$, PbO, $PbCO_3$, and Pb-substituted hydroxyapatite (Pb-HA) compared to XANES spectra collected from Ferrante rib section shown in Fig. 9 (points labeled "XAS Center" and "XAS Margin"). (Right) Difference spectra generated by subtracting the edge-step normalized μ-XANES of the "XAS Margin" point from that obtained for each reference compound and for that of "XAS Center". The residual sum of squares difference for each spectra in comparison to "XAS Margin".

which would be consistent with excretion (the elimination of toxic elements by specific excretory organs) of metabolically-absorbed mercury from the body through salivary glands. While elimination by the kidneys into urine is the primary route of excretion of toxins such as mercury, another route of elimination of heavy metal toxicants is in the feces, by the liver into the bile which enters the intestinal tract and other minor routes of excretion include saliva, sweat, mother's milk, tears and semen. There is evidence in literature that Hg is excreted by salivary glands (Berlin and Gibson, 1963; Joselow et al., 1969, 1968). Mixed with the moist environment of the mouth, Hg then deposits on teeth as a blackish patina.

In immune-compromised individuals, VL may cause gingivitis (an inflammation of the gums) and tongue ulcerations (Bosch et al., 2002), which may have been treated with mercury containing solutions. Use of these compounds in such a manner is consistent with excretion of metabolically-absorbed mercury from the body through salivary glands. These results considered along with the observed distribution of Hg in Isabella's hair may provide at least circumstantial evidence that the Hg measured was endogenously incorporated and the result of in-vivo exposure to Hg-containing compounds. Equivocally establishing the exogenous vs. endogenous nature of the Hg observed in Isabella's hair, however, would likely require analysis of additional hairs collected from different locations on the scalp.

By contrast, the most likely interpretation of the Pb measured in bone sections prepared from Ferrante II's remains is that it is endogenously incorporated and the consequence of in-life exposure to this heavy metal. The Pb is distributed throughout the bone but appears to target micro-anatomical locations consistent with bone remodeling events. Bone remodeling within human bone cortices occurs throughout life and involves the cell-based removal of cylindrical volumes and the replacement of bone around a central vascular canal. When bone is replaced, certain "bone seeking" elements, such as Pb, are incorporated into the bone mineral at a level corresponding to their serum levels (O'Flaherty, 1993). The high-resolution imaging in Fig. 9 shows that Pb is observed on canal surfaces and that many of the osteons are enriched relative to the surrounding bone. These are Pb distribution patterns that are very similar to those observed in other archaeological studies of bone using synchrotron μXRF and considered indicative of antemortem uptake and in-life exposure to Pb (Swanston et al., 2012). Other archaeological studies of bone utilizing synchrotron μXRF have also argued that the bones of individuals exposed to influx of new Pb before death would manifest as elevated concentrations in regions that exhibit the most rapid uptake, such as trabecular bone (Martin et al., 2013). The order of magnitude increase in Pb concentration at the bone margins is also similar to what has been observed by other researchers utilizing spatially-resolved elemental analysis (Meirer et al., 2011; Zoeger et al., 2005, 2006) examining in-vivo uptake of Pb along active bone mineralization fronts.

The data presented here also show that the chemical form of Pb incorporated in Ferrante's bone, as measured by X-ray absorption spectroscopy, is consistent with Pb substitution of Ca in a hydroxyapatite-like structure, as would be expected during bone growth (Meirer et al., 2011). The calculated Pb abundance for this bone, estimated from integrating the μXRF compositional maps, is between 90 and 170 ppm. These bone lead levels are consistent with those measured from powdered samples using ICP-AES and similar to Pb levels measured in bone from Isabella (this study, 110 pm) and for other Aragonese mummies (Fornaciari et al., 1989).

While it thus appears likely based on the imaging analysis presented here that Ferrante II, and circumstantially Isabella as well, may have been exposed to Pb in life for prolonged periods of time, we cannot confidently speculate how the measured levels may have contributed to the underlying medical problems reported in the historical record. Although there is currently no accepted limit for lead levels in bone as relates to neurotoxicity, researchers monitoring occupational exposure for lead workers have shown that time-integrated cumulative blood lead index correlates with

measured bone lead (Ambrose et al., 2000) and these studies may provide a sense for Ferrante II's level of exposure. For these workers, exposed to high levels of Pb over many years, mean tibial Pb concentrations generally range between 20 and 70 ppm (Ambrose et al., 2000), although some values are recorded in excess of 140 ppm. However, unlike blood lead index, lead levels in bone measure cumulative exposure. When compared to levels measured in Ferrante bone samples of 90–170 ppm, this at least suggests long-term exposure to relatively high levels of Pb for a period of years. Bone Pb concentrations of this magnitude and higher have been reported in other archaeological studies. Synchrotron XRF analysis of a fibular bone fragment from an individual interred in Antigua during the English colonial era (1793–1822) yielded Pb levels of 254 ppm (Swanston et al., 2012), higher than the levels measured here and supportive of the conclusion that this 18th century individual was exposed to Pb during life.

## 5. Conclusions

As detection sensitivity of modern analytical methods improves there has been increasing interest in utilizing these techniques in the analysis of preserved human remains for bioarchaeological investigations. However, it is also well-recognized that chemical modifications resulting from preservation practices and alterations in the burial environment have the potential for yielding anomalous results that can be analytically challenging to identify. In order to derive realistic conclusions from such results it is important to properly evaluate if the measured chemical composition reflects endogenous metals incorporated in-vivo rather than exogenous environmental contamination or alteration. The known frequent use of mercury and mercury-containing compounds in Medieval and Renaissance mummification at the very least complicates our ability to readily distinguish its endogenous incorporation in the body from that exogenously introduced during embalming. Spatially-resolved, synchrotron-based imaging and spectroscopic techniques provide archaeologists high-sensitivity, non-destructive methods that allow for sub-micrometer chemical characterization of such materials. The ability to evaluate the distribution and molecular speciation of the target elements at a near cellular length scale can clarify whether these elements are exogenous or in fact endogenously incorporated (Chevallier et al., 2006; Kakoulli et al., 2013; Kempson et al., 2006).

Previous work (Fornaciari et al., 2011, 2009) and the data presented in this study demonstrate that remains from both Ferrante II of Aragon and Isabella of Aragon contain high amounts of heavy metals; mercury and lead. But is this representative of exposure to heavy-metal compounds in life? Remains of both nobles display evidence of mercury accumulation, one on the surface of the hair and Isabella both within hair and on teeth. Spatially resolved synchrotron μXRF mapping and tomography of Isabella's hair shows a smoothly varying distribution of mercury along the hair, significantly lower Hg abundance than observed in Ferrante's hair strands and relatively uniform incorporation within the hair cortex. These observations are more consistent with metabolic absorption of mercury in life. The same cannot be asserted for mercury measured from the remains of Ferrante II. The very high levels of mercury seen in his remains, the highest concentrations of which are localized on hair and bone surfaces and the high Hg seen in retrieved embalming materials, are best explained as exogenous contamination from post-mortem embalming of the corpse. However, μXRF mapping and absorption spectroscopy of Pb measured in Ferrante's bone sections show that Pb is localized to micro-anatomical locations consistent with bone remodeling events and that it is compositionally similar to Pb-substituted hydroxyapatite and thus consistent with Pb binding in bone. We believe this is good evidence for the metabolic incorporation of lead in Ferrante's bone at levels high enough to suggest lead poisoning.

The potential for exposure of general populations in pre-industrial societies such as Renaissance Italy to heavy metals and the consequences of that exposure to their health may be underestimated. In Renaissance Europe the affluent may have been particularly vulnerable to heavy metal toxicity because of easy availability of dietary and pharmaceutical sources of heavy metals and other toxins. Trace element analysis of human remains retrieved from archaeological samples can help establish levels of exposure in comparison to modern societies. Such studies can significantly benefit from the use of high-resolution chemical imaging techniques that can help distinguish heterogeneously distributed contamination from endogenously incorporated metals.

## Acknowledgments

The study was approved by the *Soprintendenza* per *I Beni Artistici e Storici della Campania*, Naples, Italy May 22 1984, protocol # 4800. Portions of this work were performed at Beamline X26A, National Synchrotron Light Source (NSLS), Brookhaven National Laboratory. X26A is supported by the Department of Energy (DOE) - Geosciences (DE-FG02-92ER14244 to The University of Chicago - CARS). Use of the NSLS was supported by U.S. Department of Energy under Contract No. DE-AC02-98CH10886. We acknowledge Anna Trisciuoglio (University of Turin, Dept. of Veterinary Sciences) for technical support in Western Blotting analysis. Support was also provided by the 2010 Max Planck Research Award to TGB, endowed by the German Federal Ministry of Education and Research to the Max Planck Society and the Alexander von Humboldt Foundation in respect of the Hard Tissue Research Program in Human Paleobiomics. Additional funds were made available by the New Mexico Health Enhancement and Marathon Clinics Research Foundation, Albuquerque NM USA. We also wish to thank the two anonymous reviewers of this manuscript. Their insightful reviews significantly improved this work.

## Appendix A. Supplementary data

Supplementary data related to this article can be found at http://dx.doi.org/10.1016/j.jas.2014.08.019.

## References

Ambrose, T.M., Al-Lozi, M., Scott, M.G., 2000. Bone lead concentrations assessed by in vivo X-Ray fluorescence. Clin. Chem. 46, 1171–1178.
Barkley, R.A., Thompson, T.G., 1960. The total iodine and iodate-iodine content of sea-water. Deep Sea Res. 7, 24–34.
Bartkus, L., Amarasiriwardena, D., Arriaza, B., Bellis, D., Yañez, J., 2011. Exploring lead exposure in ancient Chilean mummies using a single strand of hair by laser ablation-inductively coupled plasma-mass spectrometry (LA-ICP-MS). Microchem. J. 98, 267–274.
Berlin, M., Gibson, S., 1963. Renal uptake, excretion, and retention of mercury: I. A study in the rabbit during infusion of mercuric chloride. Arch. Environ. Health Int. J. 6, 617–625.
Bertrand, L., Doucet, J., Dumas, P., Simionovici, A., Tsoucaris, G., Walter, P., 2003. Microbeam synchrotron imaging of hairs from ancient Egyptian mummies. J. Synchrotron Radiat. 10, 387–392.
Bertrand, L., Vichi, A., Doucet, J., Walter, P., Blanchard, P., 2014. The fate of archaeological keratin fibres in a temperate burial context: microtaphonomy study of hairs from Marie de Bretagne (15th c., Orléans, France). J. Archaeol. Sci. 42, 487–499.
Bianucci, R., Giuffra, V., Bachmeier, B.E., Ball, M., Pusch, C.M., Fornaciari, G., Nerlich, A.G., 2012. Eleonora of Toledo (1522–1562): evidence for tuberculosis and leishmaniasis co-infection in Renaissance Italy. Int. J. Paleopathol. 2, 231–235.
Bianucci, R., Jeziorska, M., Lallo, R., Mattutino, G., Massimelli, M., Phillips, G., Appenzeller, O., 2008. A pre-hispanic head. PLoS One 3, e2053.

Bleecker, M.L., Lindgren, K.N., Ford, D.P., 1997. Differential contribution of current and cumulative indices of lead dose to neuropsychological performance by age. Neurology 48, 639–645.
Bleecker, M.L., McNeill, F.E., Lindgren, K.N., Masten, V.L., Ford, D.P., 1995. Relationship between bone lead and other indices of lead exposure in smelter workers. Toxicol. Lett. 77, 241–248.
Bosch, R.J., Rodrigo, A.B., Sánchez, P., De Gálvez, M.V., Herrera, E., 2002. Presence of Leishmania organisms in specific and non-specific skin lesions in HIV-infected individuals with visceral leishmaniasis. Int. J. Dermatol. 41, 670–675.
Brännvall, M.-L., Bindler, R., Renberg, I., Emteryd, O., Bartnicki, J., Billström, K., 1999. The medieval metal industry was the cradle of modern large-scale atmospheric lead pollution in northern Europe. Environ. Sci. Technol. 33, 4391–4395.
Byrne, S., Amarasiriwardena, D., Bandak, B., Bartkus, L., Kane, J., Jones, J., Yañez, J., Arriaza, B., Cornejo, L., 2010. Were Chinchorros exposed to arsenic? Arsenic determination in Chinchorro mummies' hair by laser ablation inductively coupled plasma-mass spectrometry (LA-ICP-MS). Microchem. J. 94, 28–35.
Charlier, P., Poupon, J., Jeannel, G.-F., Favier, D., Popescu, S.-M., Weil, R., Moulherat, C., Huynh-Charlier, I., Dorion-Peyronnet, C., Lazar, A.-M., Hervé, C., de la Grandmaison, G.L., 2013. The embalmed heart of Richard the Lionheart (1199 A.D.): a biological and anthropological analysis. Sci. Rep. 3. Article number: 1296.
Chevallier, P., Ricordel, I., Meyer, G., 2006. Trace element determination in hair by synchrotron x-ray fluorescence analysis: application to the hair of Napoleon I. X-Ray Spectrom. 35, 125–130.
Clarkson, T.W., Magos, L., Myers, G.J., 2003. Human exposure to mercury: the three modern dilemmas. J. Trace Elem. Exp. Med. 16, 321–343.
Criss, J.W., Birks, L.S., Gilfrich, J.V., 1978. Versatile x-ray analysis program combining fundamental parameters and empirical coefficients. Anal. Chem. 50, 33–37.
D'Errico, F., Villa, F., Fornaciari, G., 1988. Dental esthetics of an Italian Renaissance noble-woman, Isabella d'Aragona. A case of chronic mercury intoxication. Ossa 13, 233–254.
Dolphin, A.E., Naftel, S.J., Nelson, A.J., Martin, R.R., White, C.D., 2013. Bromine in teeth and bone as an indicator of marine diet. J. Archaeol. Sci. 40, 1778–1786.
Drew-Bear, A., 1994. Painted Faces on the Renaissance Stage: the Moral Significance of Face-painting Conventions. Bucknell University Press.
Egeland, G.M., Ponce, R., Bloom, N.S., Knecht, R., Loring, S., Middaugh, J.P., 2009. Hair methylmercury levels of mummies of the Aleutian Islands, Alaska. Environ. Res. 109, 281–286.
Fioravanti, L., 1561. Capricci Medicinali. Lodovico Avanzo.
Fornaciari, G., 1985. The mummies of the Abbey of Saint Domenico Maggiore in Naples: a preliminary report. Arch. Antrop. Etnol. 115, 215–226.
Fornaciari, G., 2006. Le mummie aragonesi in San Domenico Maggiore di Napoli. Med. Secoli 18, 875–896.
Fornaciari, G., Ceccanti, B., Corcione, N., Bruno, J., 1989. Recherches paleonutritionnelles sur un echantillon d'une classe socialement élevée de la Renaissance italienne: la série de momies de S. Domenico Maggiore à Naples (XVe-XVIe siècles). In: Advances in Paleopathology, Proceedings of the VII European Meeting of the Paleopathology Association (Lyon, September 1988), pp. 81–87.
Fornaciari, G., Giuffra, V., Ferroglio, E., Gino, S., Bianucci, R., 2010. *Plasmodium falciparum* immunodetection in bone remains of members of the Renaissance Medici family (Florence, Italy, sixteenth century). Trans. R. Soc. Trop. Med. Hyg. 104, 583–587.
Fornaciari, G., Giuffra, V., Marinozzi, S., Picchi, M.S., Masetti, M., 2009. " Royal" pediculosis in Renaissance Italy: lice in the mummy of the King of Naples Ferdinand II of Aragon (1467–1496). Mem. Inst. Oswaldo Cruz 104, 671–672.
Fornaciari, G., Marinozzi, S., Gazzaniga, V., Giuffra, V., Picchi, M.S., Giusiani, M., Masetti, M., 2011. The use of mercury against pediculosis in the Renaissance: the case of Ferdinand II of Aragon, King of Naples, 1467–96. Med. Hist. 55, 109.
Friberg, L., Vostal, J., 1972. Mercury in the Environment: an Epidemiological and Toxicological Appraisal. CRC Press.
Joselow, M.M., Goldwater, L.J., Alvarez, A., Herndon, J., 1968. Absorption and excretion of mercury in man: XV. Occupational exposure among dentists. Arch. Environ. Health Int. J. 17, 39–43.
Joselow, M.M., Ruiz, R., Goldwater, L.J., 1969. The use of salivary (parotid) fluid in biochemical monitoring. Am. Ind. Hyg. Assoc. J. 30, 77–82.
Kakoulli, I., Prikhodko, S.V., Fischer, C., Cilluffo, M., Uribe, M., Bechtel, H.A., Fakra, S.C., Marcus, M.A., 2013. Distribution and chemical speciation of arsenic in ancient human hair using synchrotron radiation. Anal. Chem. 86, 521–526.
Kanngießer, B., 2003. Quantification procedures in micro X-ray fluorescence analysis. Spectrochim. Acta Part B Atomic Spectrosc. 58, 609–614.
Keenleyside, A., Song, X., Chettle, D.R., Webber, C.E., 1996. The lead content of human bones from the 1845 Franklin expedition. J. Archaeol. Sci. 23, 461–465.
Kempson, I.M., Chien, C.-C., Chung, C.-Y., Hwu, Y., Paterson, D., de Jonge, M.D., Howard, D.L., 2012. Fate of intravenously administered gold nanoparticles in hair follicles: follicular delivery, pharmacokinetic interpretation, and excretion. Adv. Healthc. Mater. 1, 736–741.
Kempson, I.M., Henry, D., Francis, J., 2009. Characterizing arsenic in preserved hair for assessing exposure potential and discriminating poisoning. J. Synchrotron Radiat. 16, 422–427.
Kempson, I.M., Henry, D.A., 2010. Determination of arsenic poisoning and metabolism in hair by synchrotron radiation: the case of Phar Lap. Angew. Chem. Int. Ed. 49, 4237–4240.
Kempson, I.M., Skinner, W.M., Kirkbride, K.P., 2006. Advanced analysis of metal distributions in human hair. Environ. Sci. Technol. 40, 3423–3428.
Kempson, I.M., Skinner, W.M., Kirkbride, K.P., 2007. The occurrence and incorporation of copper and zinc in hair and their potential role as bioindicators: a review. J. Toxicol. Environ. Health Part B 10, 611–622.
Kim, S.A., Punshon, T., Lanzirotti, A., Li, L., Alonso, J.M., Ecker, J.R., Kaplan, J., Guerinot, M.L., 2006. Localization of iron in Arabidopsis seed requires the vacuolar membrane transporter VIT1. Science 314, 1295–1298.
Lanzirotti, A., Sutton, S.R., Flynn, G.J., Newville, M., Rao, W., 2008. Chemical composition and heterogeneity of wild 2 cometary particles determined by synchrotron X-ray fluorescence. Meteorit. Planet. Sci. 43, 187–213.
Lanzirotti, A., Tappero, R., Schulze, D.G., 2010. Practical application of synchrotron-based hard X-Ray microprobes in soil sciences. In: Advances in Understanding Soil Environments by Application of Synchrotron-based Techniques. Elsevier, pp. 27–72.
Lindh, U., Brune, D., Nordberg, G., Wester, P.-O., 1980. Levels of antimony, arsenic, cadmium, copper, lead, mercury, selenium, silver, tin and zinc in bone tissue of industrially exposed workers. Sci. Total Environ. 16, 109–116.
Marinozzi, S., Fornaciari, G., 2005. Le mummie e l'arte medica nell'evo moderno : per una storia dell'imbalsamazione artificiale dei corpi umani nell'evo moderno. Casa Editrice Università la Sapienza, Rome.
Marsh, D., Clarkson, T., Cox, C., Myers, G., Amin-Zaki, L., Al-Tikriti, S., 1987. Fetal methylmercury poisoning: relationship between concentration in single strands of maternal hair and child effects. Arch. Neurol. 44, 1017–1022.
Martin, R.R., Naftel, S., Macfie, S., Jones, K., Nelson, A., 2013. Pb distribution in bones from the Franklin expedition: synchrotron X-ray fluorescence and laser ablation/mass spectroscopy. Appl. Phys. A 111, 23–29.
Martin, R.R., Naftel, S.J., Nelson III, A.J., S, W.D., 2007. Comparison of the distributions of bromine, lead, and zinc in tooth and bone from an ancient Peruvian burial site by X-ray fluorescence. Can. J. Chem. 85, 831–836.
Meirer, F., Pemmer, B., Pepponi, G., Zoeger, N., Wobrauschek, P., Sprio, S., Tampieri, A., Goettlicher, J., Steininger, R., Mangold, S., Roschger, P., Berzlanovich, A., Hofstaetter, J.G., Streli, C., 2011. Assessment of chemical species of lead accumulated in tidemarks of human articular cartilage by X-ray absorption near-edge structure analysis. J. Synchrotron Radiat. 18, 238–244.
Minervini, N., 1923. In: Giannotti, Tip R. (Ed.), Re Ferrandino: Studio Storico. Canossa.
Nerlich, A.G., Bianucci, R., Trisciuoglio, A., Schönian, G., Ball, M., Giuffra, V., Bachmeier, B., Pusch, C.M., Ferroglio, E., Fornaciari, G., 2012. Visceral leishmaniasis during italian renaissance, 1522–1562. Emerg. Infect. Dis. 18, 184.
Newville, M., 2014. Fundamentals of XAFS. Rev. Mineral. Geochem. 78, 33–74.
Nuttall, K.L., 2006. Interpreting hair mercury levels in individual patients. Ann. Clin. Lab. Sci. 36, 248–261.
O'Flaherty, E.J., 1993. Physiologically based models for bone-seeking elements. IV. Kinetics of lead disposition in humans. Toxicol. Appl. Pharmacol. 118, 16–29.
Olivier, G., Aaron, C., Fully, G., Tissier, G., 1978. New estimations of stature and cranial capacity in modern man. J. Hum. Evol. 7, 513–518.
Passero, G., 1780. In: Vecchion, M.M. (Ed.), Storie in forma di Giornali: presso Vincenzo Orfino, pp. 104–111.
Price, T.D., Blitz, J., Burton, J., Ezzo, J.A., 1992. Diagenesis in prehistoric bone: problems and solutions. J. Archaeol. Sci. 19, 513–529.
Punshon, T., Guerinot, M.L., Lanzirotti, A., 2009. Using synchrotron X-ray fluorescence microprobes in the study of metal homeostasis in plants. Ann. Bot. 103, 665–672.
Rasmussen, K.L., Boldsen, J.L., Kristensen, H.K., Skytte, L., Hansen, K.L., Mølholm, L., Grootes, P.M., Nadeau, M.-J., Flöche Eriksen, K.M., 2008. Mercury levels in Danish Medieval human bones. J. Archaeol. Sci. 35, 2295–2306.
Ravel, B., Newville, M., 2005. ATHENA, ARTEMIS, HEPHAESTUS: data analysis for X-ray absorption spectroscopy using IFEFFIT. J. Synchrotron Radiat. 12, 537–541.
Skerfving, S., Christoffersson, J.-O., Schütz, A., Welinder, H., Spång, G., Ahlgren, L., Mattsson, S., 1987. Biological monitoring, by in vivo XRF measurements, of occupational exposure to lead, cadmium, and mercury. Biol. Trace Elem. Res. 13, 241–251.
Sutton, S.R., Bertsch, P.M., Newville, M., Rivers, M., Lanzirotti, A., Eng, P., 2002. Microfluorescence and microtomography analyses of heterogeneous earth and environmental materials. Rev. Mineral. Geochem. 49, 429–483.
Swanston, T., Varney, T., Coulthard, I., Feng, R., Bewer, B., Murphy, R., Hennig, C., Cooper, D., 2012. Element localization in archaeological bone using synchrotron radiation X-ray fluorescence: identification of biogenic uptake. J. Archaeol. Sci. 39, 2409–2413.
Toribara, T.Y., 1995. Information from lateral scans of single hairs by X-Ray fluorescence. Instrum. Sci. Technol. 23, 217–226.
Toribara, T.Y., 2001. Analysis of single hair by XRF discloses mercury intake. Hum. Exp. Toxicol. 20, 185–188.
Trotter, M., Gleser, G.C., 1977. Corrigenda to "estimation of stature from long limb bones of American Whites and Negroes," American Journal Physical Anthropology (1952). Am. J. Phys. Anthropol. 47, 355–356.
Wheeler, H.L., Mendel, L.B., 1909. The iodine complex in sponges (3,5-Diiodtyrosine). J. Biol. Chem. 7, 1–9.
Wilson, A.S., 2005. Hair as a Bioresource in Archaeological Study. Hair in Toxicology: an Important Biomonitor. Royal Society of Chemistry, Cambridge, MA, pp. 321–345.
World Health Organization, 1972. Evaluation of Certain Food Additives and the Contaminants Mercury, Lead, and Cadmium. World Health Organization.

World Health Organization, 2008. Guidance for Identifying Populations at Risk from Mercury Exposure. World Health Organization, Geneva, Switzerland.
Zhang, J.Z., Bryce, N.S., Lanzirotti, A., Chen, C.K.J., Paterson, D., de Jonge, M.D., Howard, D.L., Hambley, T.W., 2012. Getting to the core of platinum drug biodistributions: the penetration of anti-cancer platinum complexes into spheroid tumour models. Metallomics 4, 1209–1217.
Zoger, N., Roschger, P., Hofstaetter, J.G., Jokubonis, C., Pepponi, G., Falkenberg, G., Wobrauschek, P., 2006. Lead accumulation in tidemark of articular cartilage. Osteoarthr. Cartil. 14, 906–913.
Zoeger, N., Wobrauschek, P., Streli, C., Pepponi, G., Roschger, P., Falkenberg, G., Osterode, W., 2005. Distribution of Pb and Zn in slices of human bone by synchrotron μ-XRF. X-Ray Spectrom. 34, 140–143.